Synthesis and Characterization of Pentachlorophenyl–Metal Derivatives with d^0 and d^{10} Electron Configurations

Irene Ara, Juan Forniés, M. Angeles García-Monforte, Antonio Martín, and Babil Menjón*[a]

Dedicated to Prof. Dr. Gerhard Erker for his outstanding contributions to the chemistry of Group 4 metals

Abstract: By reaction of $[TiCl_3(thf)_3]$ with LiC_6Cl_5, the homoleptic organotitanium(III) derivative $[Li(thf)_4][Ti^{III}(C_6Cl_5)_4]$ (**1**) has been prepared as a paramagnetic (d^1, $S = 1/2$, $g_{av} = 1.959(2)$), extremely air-sensitive compound. Oxidation of **1** with $[N(C_6H_4\text{-}Br\text{-}4)_3][SbCl_6]$ gives the diamagnetic (d^0) organotitanium(IV) species $[Ti^{IV}(C_6Cl_5)_4]$ (**2**). Compounds **1** and **2** are also electrochemically related ($E_{1/2} = 0.05$ V). The homoleptic, diamagnetic (d^{10}) compounds $[N(PPh_3)_2][Tl(C_6Cl_5)_4]$ (**3**) and $[Sn(C_6Cl_5)_4]$ (**4**) have also been prepared. Nearly tetrahedral environments have been found for the d^0, d^{10}, and d^1 metal centers in the molecular structures of compounds **2**–**4** as well as in that of $[Li(thf)_2(OEt_2)_2][Ti^{III}(C_6Cl_5)_4]\cdot CH_2Cl_2$ (**1′**) (X-ray diffraction). The reaction of the heavier Group 4 metal halides, MCl_4 (M = Zr, Hf) with LiC_6Cl_5 in the presence of $[NBu_4]Br$ gives, in turn, the heteroleptic species $[NBu_4][M(C_6Cl_5)_3Cl_2]$ (M = Zr (**5**), Hf (**6**)). Compounds **5** and **6** are isomorphous and isostructural, with the metal center in a trigonal-bipyramidal (*TBPY*-5) environment defined by two axial Cl ligands and three equatorial C_6Cl_5 groups (X-ray diffraction). No redox features are observed for compounds **3**–**6** in CH_2Cl_2 solution between −1.6 and +1.6 V.

Keywords: electron-deficient compounds · hafnium · pentachlorophenyl compounds · titanium · zirconium

Introduction

The effective atomic number rule (EAN, now known as the 18-electron rule)[1] was initially formulated as an extension of the octet rule, which had proven very useful in traditional main group chemistry.[2] Both rules are manifestations of the concept of closed-shell electron configuration deriving from the spherical s + p four-orbital manifold (8) or from the spherical d + s + p nine-orbital manifold (18).[3] The EAN rule found wide application in the realm of organometallic chemistry, where it is obeyed by the vast majority of chemical species, with the exception of the 16-electron square-planar d^8 species. It was, in any case, a useful tool for understanding the structure of isolable products as well as of elusive reaction intermediates.[4] Many chemical processes have been designed and many new compounds have been prepared with the helpful guidance of the EAN rule, and it is precisely this great success that discouraged research activity on organometallic species with open-shell electron configuration until recently.[5] It is now, however, well established that organo-transition-metal complexes can have a variety of electron configurations, making them not so different from classical coordination compounds. The disparity with which organometallic and coordination transition-metal compounds conform to the EAN rule has been attributed to the different crystal-field effects of the ligands involved.[6] Most organo-transition-metal derivatives contain π-stabilizing ligands located at the end of the spectroscopic series, which hence exert a strong ligand-field effect. Organo-transition-metal derivatives containing only σ-bound organic groups are comparatively much less known and they are also markedly less prone to obey the EAN rule. These σ-organyl derivatives are of fundamental importance given that they are expected to exhibit structural and reactivity properties that are qualitatively different from the more abundant related species containing π-bound ligands.

We now report on a highly unusual couple of electron-poor σ-organotitanium(III) and -titanium(IV) compounds which, in a formal sense, are nine- and eight-electron species, respectively. Our attempts to prepare analogous Zr and

[a] Dr. I. Ara, Prof. Dr. J. Forniés, Dipl.-Chem. M. A. García-Monforte, Dr. A. Martín, Dr. B. Menjón
Instituto de Ciencia de Materiales de Aragón
Facultad de Ciencias, Universidad de Zaragoza-C.S.I.C.
C/ Pedro Cerbuna 12, 50009 Zaragoza (Spain)
Fax: (+34) 976-761-187
E-mail: menjon@unizar.es

  DOI: 10.1002/chem.200400141

Hf systems are also discussed and related main-group species with closed-shell electron configurations are also given for comparison. Some of the present results have already been briefly communicated.[7]

Results and Discussion

The $[Ti^{IV}(C_6Cl_5)_4]/[Ti^{III}(C_6Cl_5)_4]^-$ system: The arylation of $[TiCl_3(thf)_3]$ with LiC_6Cl_5 in Et_2O at −78 °C, followed by the appropriate treatment, afforded $[Li(thf)_4][Ti^{III}(C_6Cl_5)_4]$ (**1**) as a yellow solid in low yield (ca. 30 %) [Eq. (1)].

$$[TiCl_3(thf)_3] + LiC_6Cl_5 \xrightarrow[2)\ thf]{1)\ Et_2O} \underset{\mathbf{1}}{[Li(thf)_4][Ti^{III}(C_6Cl_5)_4]} \quad (1)$$

Complex **1** is extremely air- and moisture-sensitive and has a rather limited thermal stability, readily decomposing above 0 °C both in solution and in the solid state. The IR spectrum of **1** shows a strong absorption at 827 cm^{-1}, assigned to the X-sensitive vibration mode of the C_6Cl_5 group.[8] Two strong absorptions associated with the thf ligand (coordinated to the Li^+ ion) are also observed at 1043 ($C-O-C_{asym}$) and 887 cm^{-1} ($C-O-C_{sym}$).[9] The MS (FAB) shows the peak corresponding to the $[Ti(C_6Cl_5)_4]^-$ ion (*m*/*z* 1036) together with some fragmentation species. All these peaks have the appropriate isotopomer distribution, which is particularly rich because of the high number of Cl atoms (^{35}Cl: 75.78(4) % and ^{37}Cl: 24.22(4) % relative natural abundance).[10] The EPR spectrum of the paramagnetic d^1 species **1** has been measured on powder samples at room temperature. The signal observed can be satisfactorily ascribed to an $S = 1/2$ system with the principal values of the *g*-tensor being $g_x = 1.985(2)$, $g_y = 1.955(2)$, and $g_z = 1.936(2)$ ($g_{av} = 1.959(2)$). These values compare well with previously reported data for Ti^{III} species.[11] No hyperfine structure stemming from the magnetically active Ti nuclei (^{47}Ti, $I = 5/2$, 7.44(2) % natural abundance; ^{49}Ti, $I = 7/2$, 5.41(2) % natural abundance)[10] is observed.

The redox behavior of **1** has been studied by electrochemical methods. The cyclic voltammogram (CV) of $[Ti^{III}(C_6Cl_5)_4]^-$, scanned at 100 mV s^{-1} from −1.6 to +1.6 and then back to −1.6 V shows a single oxidation wave ($(E_p)_{ox} = 93$ mV), which is recovered in the returning scan ($(E_p)_{red} = 4$ mV) corresponding to an electrochemically reversible semisystem ($E_{1/2} = 48.5$ mV, $\Delta E_p = 89$ mV, $i_{pa}/i_{pc} = 1.00$). It is reasonable to assign this redox process to oxidation of the metal center from Ti^{III} to Ti^{IV}. In addition, the reversibility of the process suggests that the electron exchange takes place with little change in the geometry of the coordination species. Electron-exchange processes occurring at low potentials for $[Ti(1\text{-norbornyl})_4]$ ($E_{1/2} = -1.90$ V)[12] and $[Ti(1\text{-camphenyl})_4]$ ($E_{1/2} = -1.32$ V)[13] have been attributed to $[Ti^{IV}R_4]/[Ti^{III}R_4]^-$ redox systems but, to the best of our knowledge, the reduced species were not isolated nor characterized in solution. The markedly different $E_{1/2}$ values with our **2**/**1** system can be explained in terms of the very different electron-donor abilities of the organic ligands: 1-norbornyl > 1-camphenyl ≫ C_6Cl_5, the latter really behaving as an electron-withdrawing group.[14] This electron-withdrawing ability accounts for the enhanced stabilization of the anionic $[Ti^{III}(C_6Cl_5)_4]^-$ species relative to neutral $[Ti^{IV}(C_6Cl_5)_4]$, which we sought to prepare by chemical methods.

Controlled chemical oxidation of **1** was also achieved [Eq. (2)]: the addition of solid **1** in small portions to a blue suspension of the aminium salt $[N(C_6H_4Br\text{-}4)_3][SbCl_6]$ in CH_2Cl_2 at 0 °C in 2:1 molar ratio gave the homoleptic neutral species $[Ti^{IV}(C_6Cl_5)_4]$ (**2**), which was isolated as an air-sensitive, orange solid in moderate yield.

$$\underset{\mathbf{1}}{[Li(thf)_4][Ti^{III}(C_6Cl_5)_4]} + [N(C_6H_4Br\text{-}4)_3][SbCl_6] \longrightarrow \underset{\mathbf{2}}{[Ti^{IV}(C_6Cl_5)_4]} \quad (2)$$

The required molar ratio points to the cation $[N(C_6H_4\text{-}Br\text{-}4)_3]^+$ (1.16 V versus SCE in CH_2Cl_2)[15] and the anion $[SbCl_6]^-$, both acting as oxidants.[16] The reduced antimony product was not identified. Compound **1** could also be oxidized to **2** with titrated solutions of Cl_2 in CCl_4. Compound **2** is thermally labile, decomposing rapidly at room temperature. Its scarce solubility in chlorinated hydrocarbons simplified its isolation (it precipitates in CH_2Cl_2) but precluded the possibility of obtaining good ^{13}C NMR spectroscopic data in solution. Nevertheless, a weak peak corresponding to the $[Ti(C_6Cl_5)_4]^-$ ion (*m*/*z* 1036) with the appropriate isotopomeric distribution was observed in the MS (FAB) of **2**. The most salient feature in its solid-state IR spectrum is a

Abstract in Spanish: *La reacción de $[TiCl_3(thf)_3]$ con LiC_6Cl_5, permite obtener el organoderivado homoléptico de titanio(III) $[Li(thf)_4][Ti^{III}(C_6Cl_5)_4]$ (**1**), en forma de un sólido paramagnético (d^1, S = 1/2, $g_{av} = 1.959(2)$) extremadamente sensible al aire. La oxidación de **1** con $[N(C_6H_4Br\text{-}4)_3][SbCl_6]$ da lugar al organoderivado diamagnético (d^0) de titanio(IV) $[Ti^{IV}(C_6Cl_5)_4]$ (**2**). Los compuestos **1** y **2** están también relacionados electroquímicamente ($E_{1/2} = 0.05$ V). Se han preparado a su vez, los compuestos homolépticos y diamagnéticos (d^{10}) $[N(PPh_3)_2][Tl(C_6Cl_5)_4]$ (**3**) y $[Sn(C_6Cl_5)_4]$ (**4**). Las estructuras moleculares mediante difracción de rayos X de los compuestos **2**–**4**, así como la correspondiente al derivado $[Li(thf)_2(OEt_2)_2][Ti^{III}(C_6Cl_5)_4]\cdot CH_2Cl_2$ (**1′**), evidencian entornos aproximadamente tetraédricos para los centros metálicos de configuraciones electrónicas d^0, d^{10} y d^1. Por su parte, la reacción de MCl_4 (M = Zr, Hf) con LiC_6Cl_5 en presencia de $[NBu_4]Br$ conduce a las especies heterolépticas $[NBu_4][M(C_6Cl_5)_3Cl_2]$ (M = Zr (**5**), Hf (**6**)). Cada centro metálico en los compuestos isomorfos e isoestructurales **5** y **6** tiene una geometría de bipirámide trigonal (*TBPY-5), cuyo plano ecuatorial viene definido por los grupos C_6Cl_5 y las posiciones axiales por los átomos de Cl. Los compuestos **3**–**6** no presentan comportamiento redox en CH_2Cl_2, al menos entre −1.6 y +1.6 V.*

single absorption corresponding to the X-sensitive mode of the C_6Cl_5 group,[8] which appears at a higher wavenumber than that observed in the parent compound (842 cm^{-1} in **2** versus 827 cm^{-1} in **1**). Similar shifts associated with an increase in the oxidation state of the metal center have frequently been observed in the perhalophenyl chemistry of late transition metals.[8a] No absorption could be assigned to ν(M–C) vibration modes in the IR spectra of **1** or **2**.

For decades, the chemistry of σ-organotitanium species has been virtually eclipsed by that of compounds containing π-bonded ligands (typically Cp or ligands derived thereof).[17] This occurred in spite of Ti being the first transition metal, after Pt,[18] for which a compound containing a M–C σ-bond was isolated ($[TiPh(OiPr)_3]$).[19] Recently, however, there has been an increasing interest in non-metallocene Ti compounds because of their markedly different properties and reactivity.[20] Homoleptic σ-organotitanium derivatives, $[TiR_n]^{q-}$ ($q = 0, \pm1, \pm2,\ldots$), are not just a special class of Cp-free compounds: they are archetypal chemical species, whose molecular geometry is often used as a touchstone for chemical bonding models.[21]

As far as we know, the only example to date of a $[TiR_5]^-$ stoichiometry is the methyl complex $[TiMe_5]^-$,[22] which has a trigonal-bipyramidal structure (*TBPY*-5) with strong cation–anion interactions in the salt $[Li(OEt_2)_2][TiMe_5]$.[23] Additionally, a fair number of neutral $[TiR_4]$ compounds have been isolated, in which R is most conveniently a bulky ligand in which the mechanism of β-H elimination is hindered (*e.g.* CH_2Ph,[24] CH_2CMe_3,[25] CH_2SiMe_3,[26] mesityl,[27] 1-norbornyl,[28]…). Some of these species have been used for the chemical vapor deposition of titanium or titanium carbide films.[29] Claims[30] about the isolation of "$TiMe_4$" should be viewed with great caution given recent results evidencing the ease with which Et_2O molecules enter the coordination sphere of the metal to give (*TBPY*-5)-$[TiMe_4(OEt_2)]$.[23] According to theoretical calculations, homoleptic, unsolvated "$TiMe_4$" should not exist in the presence of Et_2O, which is usually the solvent chosen to prepare it.[31] As far as we know, the only structurally characterized $[TiR_4]$ species is $[Ti(CH_2Ph)_4]$;[32] it is now generally accepted, however, that the benzyl group is not an innocent ligand, being prone to involve the π-electron density of the phenyl ring to give (η^2-benzyl)–metal coordination. $[Ti(CH_2Ph)_4]$ and its heavier homologues $[M(CH_2Ph)_4]$ (M = Zr, Hf) do, in fact, provide nice examples of η^2-benzyl coordination as a way of alleviating electronic unsaturation of the metal center.[33] To the best of our knowledge, individual well-established representatives of $[TiR_4]^-$ and $[TiR_3]$ stoichiometries have been reported to date, $Li[Ti(C_6H_2Me_3\text{-}2,4,6)_4]\cdot 4THF$[27] and $[Ti\{CH(SiMe_3)_2\}_3]$.[34] Considering the lack of structural information currently available for homoleptic σ-organotitanium(III) and titanium(IV) compounds, it would be interesting to obtain reliable data on the molecular geometry of this important class of compounds.

Single crystals of **1** were obtained from THF/*n*-hexane mixtures but they rendered only weak X-ray diffraction data. The analysis of these poor-quality data only allowed us to establish the connectivity of the atoms. Crystallization of **1** in CH_2Cl_2/Et_2O mixtures gave, in turn, good-quality crystals of $[Li(thf)_2(OEt_2)_2][Ti(C_6Cl_5)_4]\cdot CH_2Cl_2$ (**1′**) as the result of partial thf replacement by Et_2O molecules around the Li^+ cation. The crystal and molecular structures of **1′** and **2** were established by X-ray diffraction methods (Figures 1 and 2). Selected bond lengths and angles for **1′** and **2** are detailed in Tables 1 and 2, respectively. Continuous symmetry measures for the coordination environment of the Ti center have been carried out for **1′** and **2**.[35] The small values obtained ($S(T_d) = 0.98$ for **1′** and 0.27 for **2**) indicate that the two $[Ti(C_6Cl_5)_4]^{q-}$ species ($q = 0, 1$) are nearly tetrahedral.[36] There is only one crystallographically independent Ti^{IV}–C distance in **2** (211.9(6) pm) and the two independent Ti^{III}–C distances found in **1′** are identical (220.7(5) pm). The latter compare well with other known precedents of heteroleptic (σ-aryl)–Ti^{III} derivatives. The Ti^{III}–C(sp^2) distance seems to be quite insensitive to the coordination geometry and to the presence or absence of anionic π-ligands, as can be seen in the following examples: $[TiCp_2(C_6H_3Me_2\text{-}2,6)]$ (Ti–C 217.8(7) pm),[37] $[\{TiCp_2(C_6H_4Me\text{-}4)\}_2(\mu\text{-}N_2)]$ (Ti–C 221.6(7) pm),[38] $[Li(tmen)_2][TiPh_2(NiPr_2)_2]$ (Ti–C 217.3(5) and 221.0(5) pm)[39] and [Ti(acacen-κ^2O,κ^2N)($C_6H_2Me_3$-

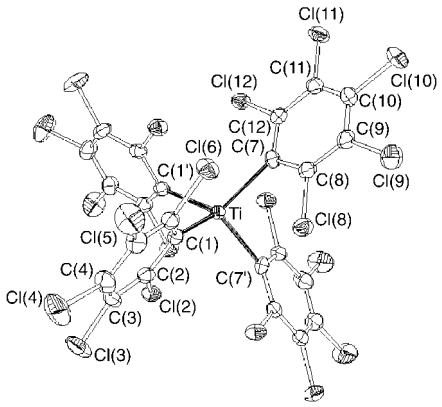

Figure 1. Structure of the anion of **1′** (thermal ellipsoid diagram; 50% probability).

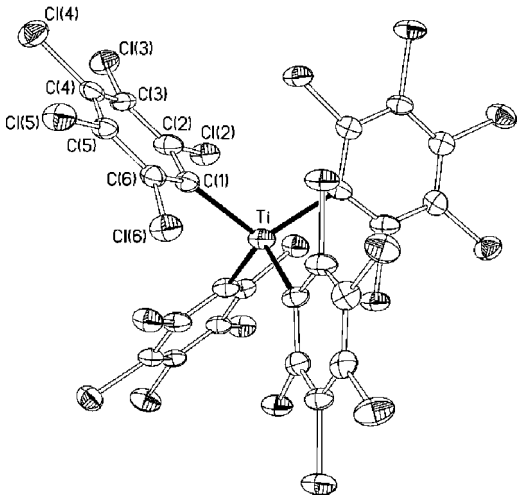

Figure 2. Structure of **2**·2 CH_2Cl_2 (thermal ellipsoid diagram; 50% probability).

Table 1. Selected interatomic distances [pm] and angles [°] and their estimated standard deviations for **1′**.

Anion			
Ti–C(1)	220.7(5)	C(1)-Ti-C(1′)	98.5(2)
Ti–C(7)	220.7(4)	C(1)-Ti-C(7)	116.8(2)
C(1)–C(2)	139.4(6)	C(1)-Ti-C(7′)	114.0(2)
C(1)–C(6)	140.6(6)	C(1′)-Ti-C(7)	114.0(2)
C(2)–Cl(2)	175.0(5)	C(1′)-Ti-C(7′)	116.8(2)
C(6)–Cl(6)	174.9(5)	C(7)-Ti-C(7′)	97.9(2)
Ti···Cl(2)	305.0(4)	Ti-C(1)-C(2)	113.0(3)
Ti···Cl(6)	377.3(4)	Ti-C(1)-C(6)	133.8(3)
C(7)–C(8)	140.0(7)	C(2)-C(1)-C(6)	113.2(4)
C(7)–C(12)	139.4(7)	C(1)-C(2)-Cl(2)	115.8(4)
C(8)–Cl(8)	175.1(5)	C(1)-C(6)-Cl(6)	118.6(4)
C(12)–Cl(12)	174.6(5)	Ti-C(7)-C(8)	114.8(3)
Ti···Cl(8)	312.6(4)	Ti-C(7)-C(12)	131.5(3)
Ti···Cl(12)	370.4(4)	C(8)-C(7)-C(12)	113.6(4)
		C(7)-C(8)-Cl(8)	116.0(3)
		C(7)-C(12)-Cl(12)	118.9(3)
Cation			
Li–O(1)	194.2(8)	O(1)-Li-O(1′)	116.8(7)
Li–O(2)	192.3(9)	O(1)-Li-O(2)	112.1(2)
O(1)–C(13)	144.6(8)	O(1)-Li-O(2′)	105.5(2)
O(1)–C(15)	141.8(8)	O(1′)-Li-O(2)	105.5(2)
O(2)–C(17)	144.4(7)	O(1′)-Li-O(2′)	112.1(2)
O(2)–C(20)	143.5(6)	O(2)-Li-O(2′)	104.2(6)
		Li-O(1)-C(13)	118.0(5)
		Li-O(1)-C(15)	129.6(6)
		Li-O(2)-C(17)	120.8(5)
		Li-O(2)-C(20)	127.1(4)

Table 2. Selected interatomic distances [pm] and angles [°] and their estimated standard deviations for **2**·2 CH_2Cl_2.

Ti–C(1)	211.9(6)	C(1)-Ti-C(1′)	112.54(16)
C(1)–C(2)	138.8(8)	C(1)-Ti-C(1″)	103.5(3)
C(1)–C(6)	139.6(8)	C(1)-Ti-C(1‴)	112.54(17)
C(2)–Cl(2)	174.0(6)	C(1′)-Ti-C(1″)	112.54(17)
C(6)–Cl(6)	171.5(6)	C(1′)-Ti-C(1‴)	103.5(3)
Ti···Cl(2)	306.7(6)	C(1″)-Ti-C(1‴)	112.54(16)
Ti···Cl(6)	365.8(6)	Ti-C(1)-C(2)	114.1(4)
		Ti-C(1)-C(6)	129.8(5)
		C(2)-C(1)-C(6)	116.1(5)
		C(1)-C(2)-Cl(2)	117.0(4)
		C(1)-C(6)-Cl(6)	121.6(5)

2,4,6)] (Ti–C22(2) pm; acacen = *N*,*N*′-ethylenebis(acetylacetone iminato) dianion).[40] The Ti^{IV}–$C(sp^2)$ distance in **2** compares well to those observed in the heteroleptic tetrahedral species [$TiPh_2(OC_6H_3Ph$-2,6$)_2$] (Ti–C 207.0(5) and 210.6(5) pm).[41] Higher electron density at the metal center achieved through: 1) dπ–pπ interaction, 2) higher coordination numbers, or 3) presence of anionic π-ligands, result in longer Ti^{IV}–$C(sp^2)$ bond lengths, as for instance in [$Ti(C_6F_5)_2(NPtBu_3)_2$] (Ti–C 219.8(3) and 220.8(3) pm),[42] [$TiPh_2(Me_2ATI)_2$] (Ti–C 217.0(3) and 218.5(3) pm; Me_2ATI = *N*,*N*′-dimethylaminotroponiminato-κ^2N),[43] and [$Ti(\eta^5$-$C_5H_4Me)_2(C_6F_5)Cl$] (Ti–C 225.9(2) pm).[44] The decrease in the Ti–C distance (by ca. 9 pm) on going from **1′** to **2** can be attributed to the increase in the oxidation state of the metal.

In spite of the regular Ti–C distances, the coordination polyhedra are not regularly tetrahedral since two of the C–Ti–C angles are smaller than expected for the ideal geometry (109.5°), while the remaining four are larger (Table 3). At first sight, this is in contrast to the VSEPR expectations, since it has been stated that: "Tetrahedral coordination is common for elements of the first transition-metal series. For d^0, d^5, and d^{10} subshells, no distortion of the tetrahedral geometry is expected".[45] If we turn from a description based on the Ti center to a description based on the polyhedron formed by the C_6Cl_5 ligands, the elongation of the tetrahedron is even more easily seen through the different size of its edges defined by the $C^{ipso}\cdots C^{ipso}$ nonbonded distances (Table 3), yielding a local D_{2d} geometry. Distortions in homoleptic ER_4 molecules (R being a polyatomic, monoanionic κ^1-ligand) have recently been rationalized in terms of the ligand close-packing (LCP) model.[46] Following this model, distortions appear because of the anisotropic character of polyatomic ligands, which makes it necessary to consider two different intramolecular contact radii for each R ligand. It is evident that aromatic rings in general and the C_6Cl_5 group in particular have a very marked anisotropy; in fact two sets of nonbonding $C^{ipso}\cdots C^{ipso}$ distances are observed, depending on the relative mutual orientation of the rings (Table 3); they depart little from 330 pm between facing rings and range from 350 to 376 pm in the remaining pairs. In every case, the plane containing each of the C_6Cl_5 rings approximately bisects one of the trigonal faces. As a result, one of the *ortho*-Cl atoms of every C_6Cl_5 group points directly to the π aromatic system of a neighbor ring, possibly incurring repulsive interactions. The minimization of this repulsion might reasonably be responsible for the swing observed in the C_6Cl_5 groups about the *ipso*-C atom, which causes the $C^{ipso}\cdots C^{para}$ vector to depart from the Ti–C^{ipso} direction, yielding two different Ti–C^{ipso}–C^{ortho} angles within each ring (**1′**: 113.0(3)° versus 133.8(3)° and 114.8(3)° versus 131.5(3)°; **2**: 115.1(4)° versus 129.8(5)°). From a geometrical point of view, the resulting geometry can be described as a tetracapped tetrahedron. The C_6Cl_5 group is known to be able to involve one of its *ortho*-Cl atoms in metal coordination, thus acting as a small-bite bidentate ligand. This coordination mode (C_6Cl_5-$\kappa C,\kappa Cl^2$) has been documented in homoleptic $[M(C_6Cl_5)_4]^{q-}$ (q = 0, 1) species of middle (Cr^{III}: d^3)[47] and late transition metals (Rh^{III} and Pt^{IV}: d^6 systems).[48,49] In all these cases, the metal coordination does not fit a tetrahedral model, being more suitably described as pseudo-octahedral. Considering that: 1) the metal coordination environments in $[Ti(C_6Cl_5)_4]^{q-}$ (q = 0, 1) only slightly depart from an ideal tetrahedron, and 2) the shorter Ti···Cl^{ortho} distances (**1′**: Ti···Cl(2) 305.0 pm, Ti···Cl(8) 312.6 pm; **2**: Ti···Cl(2) 306.7 pm) are still too long to suggest the existence of a bond—not even a secondary bonding interaction—it can be concluded that the C_6Cl_5 groups act as terminal σ-aryl ligands in **1′** and **2**. This observation is especially remarkable taking into account the high electronic unsaturation of the metal center in **1′** and **2** which, formally speaking, can be considered as nine- and eight-electron species, respectively. The organovanadium species $[V^{III}(C_6Cl_5)_4]^-$ (d^2)[50] and [$V^{IV}(C_6H_2Me_3$-2,4,6$)_4$] (d^1),[51] containing σ-bound aryl groups, were found to exhibit similar overall geometries (Table 3).

Table 3. Geometric parameters associated with the structurally characterized homoleptic aryl-metal derivatives $[MR_4]^{q-}$ of first-row transition-metals with approximately tetrahedral structure (selected main-group derivatives are also included for comparison).

Compound	Electron config.	Space group	M–C [pm]	C-M-C [°]	C···C[a] [pm]	Ref.
$[Ti^{IV}(C_6Cl_5)_4]$ (**2**)	d^0	$P\bar{4}2_1c$	211.9(6) [×4]	103.5(3) [×2]	332.8 [×2]	this work
				112.5(2) [×4]	352.5 [×4]	
$[Ti^{III}(C_6Cl_5)_4]^-$ (**1′**)	d^1	$C2/c$	220.7(5) [×4]	97.9(2)	333.5	this work
				98.5(2)	334.3	
				114.0(2) [×2]	370.3 [×2]	
				116.8(2) [×2]	375.9 [×2]	
$[V^{IV}(C_6H_2Me_3\text{-}2,4,6)_4]$	d^1	$P2_1/c$	207.1(8)	96.4(3)	309.3	TMESYV[51]
			207.3(6)	97.7(3)	313.6	
			207.5(8)	114.4(3)	348.4	
			209.5(7)	115.7(3)	351.9	
				116.2(3)	353.0	
				117.8(3)	356.9	
$[V^{III}(C_6Cl_5)_4]^-$	d^2	$Pbca$	214.2(5)	98.1(2)	325.6	OCEWIC[50]
			214.4(5)	101.2(2)	331.3	
			215.2(5)	112.1(2)	357.0	
			215.8(6)	112.6(2)	357.3	
				116.1(2)	365.0	
				117.6(2)	367.6	
$[Tl(C_6Cl_5)_4]^-$ (**3**)	d^{10}	$P2_1/c$	223.0(14)	95.7(4)	333.9	this work
			225.0(11)	97.8(5)	337.7	
			225.4(12)	114.1(5)	377.9	
			225.5(13)	115.0(5)	378.3	
				117.1(5)	382.6	
				118.6(4)	387.3	
$[Sn(C_6H_5)_4]$	d^{10}	$P2_1c$	213.9(4) [×4]	108.6(1) [×4]	347.4 [×4]	TPHESN02[56]
				111.2(2) [×2]	352.9 [×2]	
$[Sn(C_6F_5)_4]$	d^{10}	$I4_1/a$	212.6(8) [×4]	105.5(4) [×2]	338.1 [×2]	TFUPSN[57]
				111.5(2) [×4]	351.3 [×4]	
$[Sn(C_6Cl_5)_4]$ (**4**)	d^{10}	$C2/c$	216(1) [×2]	97.6(3)	326.7	this work
				99.2(4)	330.2	
			217.7(9) [×2]	114.5(4)	364.1	
				114.7(4)	365.0	
				115.5(4)	366.8	
				116.3(4)	369.8	

[a] Nonbonded distances between C-donor atoms.

The d^{10} species $[N(PPh_3)_2][Tl(C_6Cl_5)_4]$ (3) and $[Sn(C_6Cl_5)_4]$ (4): All our attempts to obtain high-quality single crystals of $[NBu_4][Tl(C_6Cl_5)_4]$[52] failed, despite both the cation and the anion being able to conform, in principle, to an S_4 symmetry site. We succeeded with the salt $[N(PPh_3)_2][Tl(C_6Cl_5)_4]$ (**3**), prepared by a simple metathetical process. Gilman and Sim reported having obtained the neutral species $[M(C_6Cl_5)_4]$ (M = Si, Sn) in very low yields (ca. 3%) by reaction of the corresponding halides MCl_4 with $Mg(C_6Cl_5)Cl$ in THF.[53] The correct formulation of these species was later questioned based on the isolation of $[M(C_6Cl_4\text{-}C_6Cl_4\text{-}\kappa C^2,\kappa C^{2'})(C_6Cl_5)_2]$ (M = Si, Ge) under similar conditions.[54] Formation of the octachlorobiphenyl-2,2′-diyl ligand was justified because of steric problems associated with the formation of the full arylated species $[M(C_6Cl_5)_4]$, "the halides R_3MX are sterically hindered towards the introduction of a fourth R group" (R = C_6Cl_5).[54] We have now prepared $[Sn(C_6Cl_5)_4]$ (**4**) in 91% yield by low temperature treatment of $[SnCl_4(thf)_2]$ with LiC_6Cl_5 in Et_2O, followed by the appropriate work-up [Eq. (3)]. This compound decomposes at 365–370 °C, a temperature range which is sufficiently different from that given by Gilman and Sim (decomp 446–449 °C)[53a] to say that the compounds under study are different.

$$[SnCl_4(thf)_2] + LiC_6Cl_5 \longrightarrow \underset{\mathbf{4}}{[Sn(C_6Cl_5)_4]} \quad (3)$$

Compounds **3** and **4** have been characterized by analytical, spectroscopic, and X-ray diffraction methods. The low-temperature crystal structure of the anion $[Tl(C_6Cl_5)_4]^-$ and that of the neutral species $[Sn(C_6Cl_5)_4]$ are shown in Figures 3 and 4, with selected bond lengths and angles detailed in Tables 4 and 5, respectively. The molecular geometries of these species can also be described as slightly elongated tetrahedra (D_{2d} symmetry), the elongation being more pronounced in **3** ($S(T_d) = 1.27$)[35] and **4** ($S(T_d) = 0.97$)[35] than in their corresponding isoleptic species **1′** and **2** (vide supra). Tetraaryl derivatives of Group 14 elements, $[ER_4]$ (R = aryl group; E = C, Si, Ge, Sn, Pb), have been thoroughly studied from both the chemical and structural point of view.[55] Amongst the many known $[SnR_4]$ representatives, the structural features of $[SnPh_4]$[56] and $[Sn(C_6F_5)_4]$[57] seemed particularly relevant to us because of their obvious relationship with **4** (Table 3). The first coordination sphere of Sn in $[SnPh_4]$ is a virtually perfect tetrahedron with a very narrow range of C–M–C angles (108.6(1)° and 111.2(2)°) and almost identical edge lengths ($C^{ipso}\cdots C^{ipso}$ 347.4 and

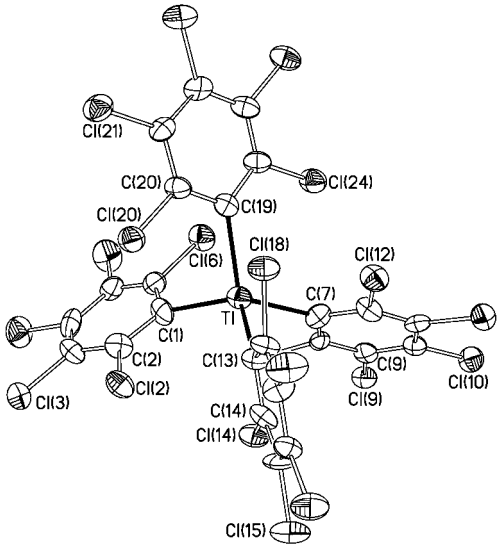

Figure 3. Structure of the anion of $\mathbf{3}\cdot 0.75\,CH_2Cl_2\cdot 0.5\,C_6H_{14}$ (thermal ellipsoid diagram; 50% probability).

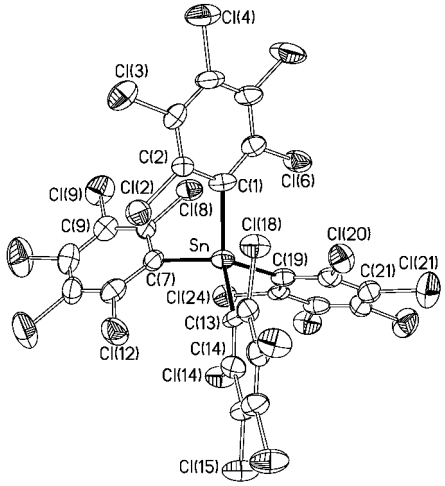

Figure 4. Structure of $\mathbf{4}\cdot 0.25\,C_2Cl_4$ (thermal ellipsoid diagram; 50% probability).

352.9 pm). Little structural change is observed in the molecular geometry of the perfluorinated species $[Sn(C_6F_5)_4]$, not even in the Sn–C bond lengths (212.6(8) versus 213.9(4) pm), in spite of the different electron-withdrawing ability attributed to the Ph and the C_6F_5 groups.[58] $[SnPh_4]$ and $[Sn(C_6F_5)_4]$ crystallize in tetragonal space groups ($P\bar{4}2_1c$ and $I4_1/a$, respectively) with the Sn atoms located on S_4 symmetry sites, as seems to be the tendency of $[ER_4]$ molecules when there is no energy penalty associated.[55a] The fact that **1′** and **3** crystallize in nontetragonal space groups ($C2/c$ and $P2_1/c$, respectively) could be attributed to the inappropriate symmetry of the cations $[Li(thf)_2(OEt_2)_2]^+$ and $[N(PPh_3)_2]^+$. There is no obvious reason, however, why $[Ti(C_6Cl_5)_4]$ (**2**) crystallizes in the tetragonal $P\bar{4}2_1c$ space group, while its isoleptic species $[Sn(C_6Cl_5)_4]$ (**4**) crystallises in the $C2/c$ group. The Sn–C distances in **4** (216(1) and 218(1) pm) are slightly longer than in $[SnPh_4]$ and in $[Sn(C_6F_5)_4]$ (Table 3). The C-Sn-C angles are between 97.6(3)° and 116.3(4)°, defining an elongated tetrahedron with edges ranging from 326.7 to 369.8 pm. A wider range for $C^{ipso}\cdots C^{ipso}$ nonbonded distances (between 333.9 and 387.3 pm) is observed in the anion $[Tl(C_6Cl_5)_4]^-$, in keeping with a wider range of C-M-C

Table 4. Selected interatomic distances [pm] and angles [°] and their estimated standard deviations for the anion of $\mathbf{3}\cdot 0.75\,CH_2Cl_2\cdot 0.5\,C_6H_{14}$.

Tl–C(1)	223.0(14)	C(1)-Tl-C(7)	117.1(5)
Tl–C(7)	225.5(13)	C(1)-Tl-C(13)	115.0(5)
Tl–C(13)	225.0(11)	C(1)-Tl-C(19)	97.8(5)
Tl–C(19)	225.4(12)	C(7)-Tl-C(13)	95.7(4)
C(1)–C(2)	138.7(17)	C(7)-Tl-C(19)	114.1(5)
C(1)–C(6)	140.1(18)	C(13)-Tl-C(19)	118.6(4)
C(2)–Cl(2)	172.1(13)	Tl-C(1)-C(2)	125.3(10)
C(6)–Cl(6)	174.9(13)	Tl-C(1)-C(6)	119.9(9)
Tl···Cl(2)	354.6(3)	C(2)-C(1)-C(6)	114.7(12)
Tl···Cl(6)	337.8(3)	C(1)-C(2)-Cl(2)	119.8(10)
C(7)–C(8)	141.0(16)	C(1)-C(6)-Cl(6)	118.8(11)
C(7)–C(12)	137.1(18)	Tl-C(7)-C(8)	124.6(10)
C(8)–Cl(8)	174.5(13)	Tl-C(7)-C(12)	120.7(9)
C(12)–Cl(12)	174.2(11)	C(8)-C(7)-C(12)	114.2(11)
Tl···Cl(8)	355.3(3)	C(7)-C(8)-Cl(8)	119.0(10)
Tl···Cl(12)	337.2(4)	C(7)-C(12)-Cl(12)	118.1(10)
C(13)–C(14)	138.8(16)	Tl-C(13)-C(14)	118.2(8)
C(13)–C(18)	139.4(15)	Tl-C(13)-C(18)	126.5(8)
C(14)–Cl(14)	173.6(12)	C(14)-C(13)-C(18)	114.7(11)
C(18)–Cl(18)	175.4(11)	C(13)-C(14)-Cl(14)	119.3(10)
Tl···Cl(14)	334.2(3)	C(13)-C(18)-Cl(18)	118.2(9)
Tl···Cl(18)	357.0(3)	Tl-C(19)-C(20)	118.5(9)
C(19)–C(20)	138.3(16)	Tl-C(19)-C(24)	125.8(9)
C(19)–C(24)	140.8(16)	C(20)-C(19)-C(24)	115.0(11)
C(20)–Cl(20)	174.6(12)	C(19)-C(20)-Cl(20)	119.7(9)
C(24)–Cl(24)	174.5(13)	C(19)-C(24)-Cl(24)	118.0(9)
Tl···Cl(20)	336.1(3)		
Tl···Cl(24)	356.3(3)		

Table 5. Selected interatomic distances [pm] and angles [°] and their estimated standard deviations for $\mathbf{4}\cdot 0.25\,C_2Cl_4$.

Sn–C(1)	217.7(9)	C(1)-Sn-C(7)	99.2(4)
Sn–C(7)	216.0(10)	C(1)-Sn-C(13)	116.3(4)
Sn–C(13)	217.7(9)	C(1)-Sn-C(19)	114.5(4)
Sn–C(19)	216.3(10)	C(7)-Sn-C(13)	115.5(4)
C(1)–C(2)	140.3(12)	C(7)-Sn-C(19)	114.7(4)
C(1)–C(6)	137.8(13)	C(13)-Sn-C(19)	97.6(3)
C(2)–Cl(2)	174.4(9)	Sn-C(1)-C(2)	117.1(7)
C(6)–Cl(6)	172.5(10)	Sn-C(1)-C(6)	125.7(7)
Sn···Cl(2)	326.5(3)	C(2)-C(1)-C(6)	116.9(9)
Sn···Cl(6)	351.9(3)	C(1)-C(2)-Cl(2)	118.9(8)
C(7)–C(8)	136.6(12)	C(1)-C(6)-Cl(6)	119.9(8)
C(7)–C(12)	142.4(13)	Sn-C(7)-C(8)	119.3(7)
C(8)–Cl(8)	171.4(10)	Sn-C(7)-C(12)	124.6(7)
C(12)–Cl(12)	173.4(10)	C(8)-C(7)-C(12)	115.9(9)
Sn···Cl(8)	329.15(25)	C(7)-C(8)-Cl(8)	119.5(8)
Sn···Cl(12)	353.5(3)	C(7)-C(12)-Cl(12)	120.2(8)
C(13)–C(14)	136.5(12)	Sn-C(13)-C(14)	117.8(7)
C(13)–C(18)	141.2(12)	Sn-C(13)-C(18)	124.4(7)
C(14)–Cl(14)	172.0(10)	C(14)-C(13)-C(18)	117.6(9)
C(18)–Cl(18)	172.6(10)	C(13)-C(14)-Cl(14)	120.1(7)
Sn···Cl(14)	327.2(3)	C(13)-C(18)-Cl(18)	120.5(7)
Sn···Cl(18)	352.9(3)	C(20)-C(19)-C(24)	116.0(9)
C(19)–C(20)	137.6(12)	Sn-C(19)-C(20)	118.1(7)
C(19)–C(24)	139.7(13)	Sn-C(19)-C(24)	125.7(8)
C(20)–Cl(20)	172.4(10)	C(19)-C(20)-Cl(20)	119.5(8)
C(24)–Cl(24)	173.9(10)	C(19)-C(24)-Cl(24)	119.9(8)
Sn···Cl(20)	327.1(3)		
Sn···Cl(24)	353.6(3)		

angles (C-Tl-C 95.7(4)–118.6(4)°). The Tl–C distances in **3** (223.0(14) and 225.5(13) pm) are longer than those found in other four-coordinate perhaloaryl thallium(III) derivatives, like in neutral $[Tl(C_6F_5)_3(OPPh_3)]$ (Tl–C 218.0(4)–219.2(4) pm)[59] or in the anionic species $[Tl(C_6F_5)_2Cl_2]^-$ (Tl–C 216.7(7) and 217.7(7) pm).[59] Tl–C bond lengths ranging from 216.9(9) to 222.4(9) pm were found in the homoleptic, three-coordinate compound $[Tl(C_6H_2Me_3\text{-}2,4,6)_3]$.[60] Long M···Cl^{ortho} distances are observed in **3** and **4** (Table 4 and Table 5), suggesting that they are to be considered as non-bonded distances. Less marked swings of the C_6Cl_5 rings are observed in **3** and **4** than in their corresponding isoleptic titanium derivatives **1**′ and **2**.

The IR spectra of **3** and **4** show single absorptions at 826 and 846 cm^{-1} respectively, assignable to the only IR active X-sensitive vibration mode[8] expected for tetrahedral $[E(C_6Cl_5)_4]^{q-}$ species ($q = 0, 1$; T_d, IR active Γ_{M-C} fundamentals: F_2).

The Zr and Hf compounds: The low-temperature treatment of $ZrBr_4$ or HfI_4 with LiC_6Cl_5 in Et_2O gave no reaction since, in both cases, unaltered starting material was recovered from the reaction medium in nearly quantitative yield. The reaction of MCl_4 (M = Zr, Hf) with LiC_6Cl_5 under similar conditions afforded lithium-containing mixtures from which no well-defined product could be isolated. Considering the possibility that anionic complex species could have formed, $[NBu_4]Br$ was added after the arylation process and, by so doing, the heteroleptic compounds $[NBu_4][M(C_6Cl_5)_3Cl_2]$ (M = Zr (**5**), Hf (**6**)) could be isolated in about 70% yield [Eq. (4)]. No halide replacement (Cl^- by Br^-) was observed in the final product.

$$MCl_4 + LiC_6Cl_5 \xrightarrow{+\,[NBu_4]Br} [NBu_4][M(C_6Cl_5)_3Cl_2] \quad (4)$$

5, M = Zr
6, M = Hf

Interestingly, the reaction of $ZrCl_4$ with LiC_6F_5 has recently been reported to also proceed with partial arylation; in this case, salts of the more negatively charged anions [(*OC*-6-12)-$Zr(C_6F_5)_4Cl_2]^{2-}$ and [(*PBPY*-7-11)-$Zr(C_6F_5)_5F_2]^{3-}$ were obtained depending on the specific reaction conditions.[61] Compounds **5** and **6** were identified by analytical, spectroscopic, and X-ray diffraction methods. They are isomorphous and virtually isostructural with very similar cell dimensions and volume (Table 8). The molecular structures of the anions $[M(C_6Cl_5)_3Cl_2]^-$ as found in crystals of **5**·0.75 CH_2Cl_2 and **6**·0.5 CH_2Cl_2 are jointly depicted in Figure 5. Selected bond lengths and angles are to be found in Tables 6 and 7. The metal atoms are in trigonal bipyramidal (*TBPY*-5) environments, as evidenced by the near-to-unit values of the angular structural parameter, τ, of 0.905 for **5** and 0.913 for **6**.[62] The axial positions are occupied by the Cl atoms and the C_6Cl_5 groups in the trigonal equatorial plane are tilted and hellicoidally arranged around the Cl–M–Cl axes. This (*TBPY*-5-11) geometry is in keeping with the appearance of single absorptions in the IR spectra of **5**

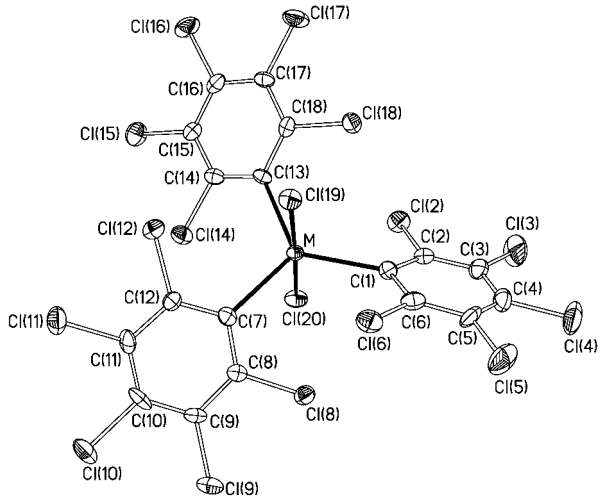

Figure 5. Structure of the anions $[M(C_6Cl_5)_3Cl_2]^-$ of **5**·0.75 CH_2Cl_2 (M = Zr) and **6**·0.5CH_2Cl_2 (M = Hf) (thermal ellipsoid diagram; 50% probability).

Table 6. Selected interatomic distances [pm] and angles [°] and their estimated standard deviations for the anion of **5**·0.75 CH_2Cl_2.

Zr–C(1)	229.6(6)	Cl(19)-Zr-Cl(20)	177.49(7)
Zr–C(7)	233.8(7)	C(1)-Zr-C(7)	121.2(2)
Zr–C(13)	232.8(7)	C(1)-Zr-C(13)	123.2(2)
Zr–Cl(19)	241.55(18)	C(7)-Zr-C(13)	115.6(2)
Zr–Cl(20)	241.65(18)	Cl(19)-Zr-C(1)	92.17(17)
C(1)–C(2)	139.4(9)	Cl(19)-Zr-C(7)	90.86(17)
C(1)–C(6)	139.0(10)	Cl(19)-Zr-C(13)	87.66(16)
C(2)–Cl(2)	175.9(7)	Cl(20)-Zr-C(1)	90.26(17)
C(6)–Cl(6)	174.8(8)	Cl(20)-Zr-C(7)	88.38(17)
C(7)–C(8)	136.9(9)	Cl(20)-Zr-C(13)	90.51(16)
C(7)–C(12)	138.9(9)	Zr-C(1)-C(2)	122.6(5)
C(8)–Cl(8)	174.6(7)	Zr-C(1)-C(6)	123.2(5)
C(12)–Cl(12)	174.4(7)	C(2)-C(1)-C(6)	114.0(6)
C(13)–C(14)	141.0(9)	Zr-C(7)-C(8)	120.6(5)
C(13)–C(18)	138.1(9)	Zr-C(7)-C(12)	123.6(5)
C(14)–Cl(14)	173.8(7)	C(8)-C(7)-C(12)	115.6(6)
C(18)–Cl(18)	174.9(7)	Zr-C(13)-C(14)	123.1(5)
		Zr-C(13)-C(18)	121.5(5)
		C(14)-C(13)-C(18)	114.8(6)

Table 7. Selected interatomic distances [pm] and angles [°] and their estimated standard deviations for the anion of **6**·0.5 CH_2Cl_2.

Hf–C(1)	225.9(13)	Cl(19)-Hf-Cl(20)	177.68(13)
Hf–C(7)	229.7(13)	C(1)-Hf-C(7)	122.9(5)
Hf–C(13)	230.6(13)	C(1)-Hf-C(13)	121.7(5)
Hf–Cl(19)	240.0(3)	C(7)-Hf-C(13)	115.4(5)
Hf–Cl(20)	240.2(3)	Cl(19)-Hf-C(1)	90.0(3)
C(1)–C(2)	144.0(19)	Cl(19)-Hf-C(7)	90.5(3)
C(1)–C(6)	142(2)	Cl(19)-Hf-C(13)	88.7(3)
C(2)–Cl(2)	174.5(16)	Cl(20)-Hf-C(1)	92.2(3)
C(6)–Cl(6)	173.2(14)	Cl(20)-Hf-C(7)	87.8(3)
C(7)–C(8)	137.3(19)	Cl(20)-Hf-C(13)	90.7(3)
C(7)–C(12)	140.4(19)	Hf-C(1)-C(2)	124.3(10)
C(8)–Cl(8)	174.9(15)	Hf-C(1)-C(6)	123.2(10)
C(12)–Cl(12)	174.6(15)	C(2)-C(1)-C(6)	112.3(12)
C(13)–C(14)	139.0(19)	Hf-C(7)-C(8)	121.6(10)
C(13)–C(18)	140.4(18)	Hf-C(7)-C(12)	123.7(9)
C(14)–Cl(14)	173.4(13)	C(8)-C(7)-C(12)	114.2(12)
C(18)–Cl(18)	173.0(14)	Hf-C(13)-C(14)	124.9(10)
		Hf-C(13)-C(18)	119.7(10)
		C(14)-C(13)-C(18)	115.0(12)

(321 cm^{-1}) and **6** (295 cm^{-1}), attributable to ν(M–Cl) (D_{3h}, IR active Γ_{M-Cl} fundamentals: A_2''). Single absorptions assignable to the X-sensitive vibration modes of the C_6Cl_5 groups[8] are also observed in the IR spectra of **5** (at 833 cm^{-1}) and **6** (at 834 cm^{-1}), in agreement with symmetry expectations (D_{3h}, IR active Γ_{M-C} fundamentals: E'). A defined absorption could not, however, be assigned to ν(M–C). The Zr–Cl bond lengths (ca. 242(2) pm) do not significantly depart from those found for instance in $[ZrCp_2Cl_2]$ (Zr–Cl 243.6(5) and 244.6(5) pm).[63] The Zr–C_6Cl_5 distances in **5** (Zr–C 229.6(6)–233.8(7) pm) are also similar to the Zr–C_6H_5 distances found in $[ZrCp_2Ph_2]$ (Zr–C 229.7(2) and 230.4(2) pm).[64] The recently reported crystal structure of $[Zr(CH_2CMe_3)_3Cl]$ reveals a polymeric chain structure $[\{Zr(CH_2CMe_3)_3(\mu\text{-}Cl)\}_\infty]$ made of TBPY-5 ···Cl–$Zr(CH_2CMe_3)_3$–Cl··· units.[65] The significantly longer axial Zr–Cl distances (254.7(1) pm) found in the polymeric compound can be explained by the bridging function of the Cl atoms and the shorter equatorial Zr–C distances (ca. 219.9(4) pm) may be due to the neutral character of the complex species. Apart from these understandable differences, the overall geometries around the Zr centers in the polymeric (R = CH_2CMe_3) and discrete (R = C_6Cl_5) "Cl–ZrR_3–Cl" species are rather similar. Compound **6** shows virtually the same structural features as **5** with slightly shorter M–Cl and M–C distances for Hf than for Zr. This is a normal observation in the organometallic chemistry of these metals and has been attributed to the slightly smaller size of Hf.[66]

The electrochemical behavior of **5** and **6** was studied by cyclic voltammetry, but no defined electron exchange process was observed between −1.6 and +1.6 V in CH_2Cl_2 solution.

Concluding Remarks

The highly unusual organotitanium derivatives $[Li(thf)_4][Ti^{III}(C_6Cl_5)_4]$ (**1**) and $[Ti^{IV}(C_6Cl_5)_4]$ (**2**) have been prepared and characterized. These species are related by an electrochemically reversible one-electron redox process, occurring at near-zero potential ($E_{1/2}$ = 0.05 V in CH_2Cl_2 solution). The crystal structures of $[Li(thf)_2(OEt_2)_2][Ti^{III}(C_6Cl_5)_4]$ (**1′**) and **2** have been established by X-ray diffraction methods, thus providing, for the first time, unequivocal structural information about homoleptic σ-organotitanium(III) and -titanium(IV) compounds. High-yield procedures to prepare $[N(PPh_3)_2][Tl(C_6Cl_5)_4]$ (**3**) and $[Sn(C_6Cl_5)_4]$ (**4**) have also been devised and their crystal structures have been determined for comparison purposes. Our attempts to obtain similar homoleptic Zr and Hf derivatives gave instead the five-coordinate compounds $[NBu_4][(TBPY\text{-}5\text{-}11)\text{-}M(C_6Cl_5)_3Cl_2]$ (M = Zr (**5**), Hf (**6**)) as the result of partial arylation. The metal coordination environments found in compounds **1′**–**4** can be described—regardless of their different electron configurations—as elongated tetrahedra (D_{2h} symmetry). Growing distortions are found for the $[M(C_6Cl_5)_4]^{q-}$ species (q = 0, 1) as follows: **2** (Ti^{IV}: d^0) < **4** (Sn^{IV}: d^{10}) ≈ **1′** (Ti^{III}: d^1) < **3** (Tl^{III}: d^{10}). In all cases, the swing observed in the C_6Cl_5 rings can be attributed to steric problems associated with the nearly tetrahedral packing of these ligands around the metal center. No evidence has been found suggesting the existence of additional secondary bonding interactions between the metal and any of the *ortho*-Cl atoms of the C_6Cl_5 groups. All these structural features allow us to consider the main-group derivatives **3** and **4** as 18-electron species, while the organotitanium compounds **1** and **2** can be viewed as highly unsaturated nine- and eight-electron species, respectively. Any π contribution to the Ti^{IV}–C_6Cl_5 bond in the most unsaturated species **2** can be considered as negligible because 1) the marked electron-withdrawing character of the C_6Cl_5 group[14] would inhibit any additional π-donation from the ligand, and 2) the lack of d electrons on titanium (d^0) makes the metal-to-ligand π-backbonding mechanism impossible.

Experimental Section

General: All reactions and manipulations were carried out under purified argon using Schlenk techniques. Solvents were dried by standard methods and distilled prior to use. The starting materials $[TiCl_3(thf)_3]$,[67] $[SnCl_4(thf)_2]$,[68] $[NBu_4][Tl(C_6Cl_5)_4]$,[52] LiC_6Cl_5,[69] and $[N(PPh_3)_2]Cl$[70] were prepared as described elsewhere. The aminium salt $[N(C_6H_4Br\text{-}4)_3][SbCl_6]$ and the metal halides MCl_4 (M = Ti, Zr, Hf) were purchased (Aldrich) and used as received. Elemental analyses were carried out with a Perkin–Elmer 2400-Series II microanalyzer. IR spectra of KBr discs were recorded on the following Perkin–Elmer spectrophotometers: 883 (4000–200 cm^{-1}) or Spectrum One (4000–350 cm^{-1}). NMR spectra were recorded on a Varian Unity-300 spectrometer. Unless otherwise stated, the spectroscopic measurements were carried out at room temperature. Mass spectra were recorded on a VG-Autospec spectrometer using the standard Cs-ion FAB (acceleration voltage: 35 kV). Electrochemical studies were carried out using an EG&G model 273 potentiostat in conjunction with a three-electrode cell, in which the working electrode was a platinum disc, the auxiliary electrode a platinum wire, and the reference an aqueous saturated calomel electrode (SCE) separated from the test solution by a fine-porosity frit and an agar bridge saturated with KCl. Where possible, solutions were 5×10^{-4} mol dm^{-3} in the test compound and 0.1 mol dm^{-3} in $[NBu_4][PF_6]$ as the supporting electrolyte. At the end of each voltammetric experiment, $[Fe(\eta^5\text{-}C_5H_5)_2]$ was added to the solution as an internal standard for potential measurements. Under the conditions used, the E^o value for the couple $[Fe(\eta^5\text{-}C_5H_5)_2]^+$–$[Fe(\eta^5\text{-}C_5H_5)_2]$ was 0.47 V.

Synthesis of $[Li(thf)_4][Ti^{III}(C_6Cl_5)_4]$ (1): A cooled suspension of $[TiCl_3(thf)_3]$ (2.37 g, 6.40 mmol) in Et_2O (15 mL) was slowly added by cannula to a solution of LiC_6Cl_5 (ca. 32 mmol) in Et_2O (70 mL) at −78 °C. The mixture was allowed to warm up to 0 °C and was stirred in an ice bath for 3.5 h. By then, an orange solid had formed, which was filtered off and treated with CH_2Cl_2 (70 mL) at 0 °C. The extract was evaporated to dryness and the resulting residue was redissolved in thf (10 mL) and filtered. The diffusion of Et_2O (50 mL) overlaid on the preceding solution at −30 °C caused the crystallization of **1** as an orange solid that turned yellow when vacuum dried (2.76 g, 2.06 mmol; 32 % yield). Crystals suitable for X-ray diffraction analysis with formula $[Li(thf)_2(OEt_2)_2][Ti(C_6Cl_5)_4]\cdot CH_2Cl_2$ (**1′**) were obtained by slow diffusion of a layer of Et_2O (30 mL) into a solution of **1** (50 mg) in CH_2Cl_2 (10 mL) at −30 °C. IR (KBr): $\tilde{\nu}_{max}$ = 1507 (m), 1461 (m), 1312 (s), 1283 (vs), 1224 (m), 1141 (m), 1063 (s), 1043 (s; C-O-C_{asym}),[9] 887 (m; C-O-C_{sym}),[9] 827 (vs; C_6Cl_5: X-sensitive vibration),[8] 666 cm^{-1} (vs); MS (FAB): m/z: 1036 $[Ti(C_6Cl_5)_4]^-$, 824 $[Ti(C_6Cl_5)_3Cl]^-$, 577 $[Ti(C_6Cl_5)_2Cl]^-$, 365 $[Ti(C_6Cl_5)Cl_2]^-$; elemental analysis calcd (%) for $C_{40}H_{32}Cl_{20}LiO_4Ti$: C 35.8, H 2.4; found: C 36.6, H 2.3.

Synthesis of $[Ti^{IV}(C_6Cl_5)_4]$ (2): Solid **1** (1.72 g, 1.28 mmol) was added in small portions to a suspension of $[N(C_6H_4Br\text{-}4)_3][SbCl_6]$ (0.52 g, 0.64 mmol) in CH_2Cl_2 (10 mL) at 0 °C (ice bath). The initially blue suspension changed gradually to orange. After the mixture had been stirred

for 30 min at the same temperature, the orange solid was filtered, washed with CH_2Cl_2 (3×3 mL), and vacuum dried (**2**: 0.57 g, 0.55 mmol; 43% yield). Crystals suitable for X-ray diffraction analysis were obtained in situ by slow diffusion of a CH_2Cl_2 solution of Cl_2 overlaid on another CH_2Cl_2 solution of **1** at −30 °C. IR (KBr): $\tilde{\nu}_{max}$ = 1502 (m), 1396 (m), 1322 (s), 1315 (s), 1289 (vs), 1150 (s), 1075 (s), 842 (s; C_6Cl_5: X-sensitive vibration),[8] 740 (w), 678 cm^{-1} (s); MS (FAB): *m/z*: 1036 $[Ti(C_6Cl_5)_4]^-$; elemental analysis calcd (%) for $C_{24}Cl_{20}Ti$: C 27.6; found: C 27.25.

Synthesis of $[N(PPh_3)_2][Tl(C_6Cl_5)_4]$ (3): $[N(PPh_3)_2]Cl$ (0.82 g, 1.43 mmol) was added to a solution of $[NBu_4][Tl(C_6Cl_5)_4]$ (1.04 g, 0.72 mmol) in CH_2Cl_2 (25 mL). After 30 min of stirring, the mixture was concentrated by evaporation. Addition of *i*PrOH (30 mL) caused the precipitation of an off-white solid, which was washed with *i*PrOH (3×10 mL) and Et_2O (3×3 mL), and vacuum dried (**3**: 1.13 g, 0.65 mmol; 90% yield). Crystals suitable for X-ray diffraction analysis were obtained by slow diffusion of a layer of *n*-hexane (10 mL) into a solution of **3** (15 mg) in CH_2Cl_2 (3 mL) at −30 °C. IR (KBr): $\tilde{\nu}_{max}$ = 1438 (m), 1316 (s), 1289 (vs), 1264 (sh), 1184 (w), 1147 (w), 1115 (m; $[N(PPh_3)_2]^+$), 1061 (w), 998 (w), 826 (m; C_6Cl_5: X-sensitive vibr.),[8] 745 (w; $[N(PPh_3)_2]^+$), 723 (m; $[N(PPh_3)_2]^+$), 691 (m; $[N(PPh_3)_2]^+$), 670 (m), 547 (m; $[N(PPh_3)_2]^+$), 534 (m; $[N(PPh_3)_2]^+$), 500 cm^{-1} (m; $[N(PPh_3)_2]^+$); MS (FAB): *m/z*: 1193 $[Tl(C_6Cl_5)_4]^-$, 981 $[Tl(C_6Cl_5)_3Cl]^-$, 769 $[Tl(C_6Cl_5)_2Cl_2]^-$, 557 $[Tl(C_6Cl_5)Cl_3]^-$; elemental analysis calcd (%) for $C_{60}H_{30}Cl_{20}NP_2Tl$: C 41.4, H 1.7, N 0.8; found: C 40.4, H 1.4, N 0.8.

Synthesis of $[Sn(C_6Cl_5)_4]$ (4): $[SnCl_4(thf)_2]$ (0.70 g, 1.73 mmol) was added to a solution of LiC_6Cl_5 (ca. 10 mmol) in Et_2O (60 mL) at −78 °C. The suspension was allowed to warm up to room temperature and, after 15 h of stirring, the white solid was filtered, washed with Et_2O (3×7 mL) and MeOH (3×15 mL), and vacuum dried (**4**: 1.76 g, 1.58 mmol; 91% yield). Crystals suitable for X-ray diffraction analysis were obtained by slow evaporation of a saturated $CCl_2{=}CCl_2$ solution of **4** at room temperature. ^{13}C NMR ($CCl_2{=}CCl_2$):[71] δ = 147.97 (*ipso*-C), 139.23, 136.21 (*p*-C), 133.35; ^{119}Sn NMR ($CCl_2{=}CCl_2$):[71] δ = −141.0; IR (KBr): $\tilde{\nu}_{max}$ = 1510 (m), 1336 (s), 1325 (vs), 1299 (vs), 1202 (w), 1170 (m), 1082 (m), 846 (s; C_6Cl_5: X-sensitive vibr.),[8] 712 (w), 682 (s), 620 cm^{-1} (w); MS (FAB): *m/z*: 861 $[Sn(C_6Cl_5)_3]^+$, 649 $[Sn(C_6Cl_5)_2Cl]^+$; elemental analysis calcd (%) for $C_{24}Cl_{20}Sn$: C 25.8; found: C 26.65.

Synthesis of $[NBu_4][Zr(C_6Cl_5)_3Cl_2]$ (5): $ZrCl_4$ (0.77 g, 3.30 mmol) was added to a solution of LiC_6Cl_5 (ca. 23 mmol) in Et_2O (50 mL) at −78 °C and the resulting suspension was allowed to warm up to −30 °C. At this temperature, $[NBu_4]Br$ (1.06 g, 3.30 mmol) was further added and the mixture was allowed to reach 0 °C. After the mixture had been stirred for 3 h, the light brown solid in suspension was filtered off, washed with Et_2O (3×7 mL) and vacuum dried. The solid was treated with CH_2Cl_2 (50 mL) at 0 °C and the extract was filtered and concentrated to about 10 mL. Addition of a Et_2O layer (40 mL) on the preceding solution and subsequent diffusion at −30 °C gave a brown solid, which was filtered off, washed with Et_2O (3×5 mL), and vacuum dried (**5**: 2.66 g, 2.30 mmol; 70% yield). Crystals suitable for X-ray diffraction analysis were obtained by slow diffusion of a layer of *n*-hexane (15 mL) into a solution of **5** (40 mg) in CH_2Cl_2 (6 mL) at −30 °C. ^{13}C NMR ([^{2}H]chloroform, −20 °C):[72] δ = 180.12 (*ipso*-C), 138.02, 131.56 (*p*-C), 129.80; IR (KBr): $\tilde{\nu}_{max}$ = 1509 (m), 1480 (m), 1470 (m), 1396 (m), 1381 (m), 1324 (m), 1314 (s), 1284 (vs), 1221 (w), 1167 (w), 1146 (m), 1067 (s), 876 (w; NBu_4^+), 833 (s; C_6Cl_5: X-sensitive vibr.),[8] 739 (w; NBu_4^+), 670 (s), 321 cm^{-1} (m; Zr−Cl); MS (FAB): *m/z*: no peaks were observed; elemental analysis calcd (%) for $C_{34}H_{36}Cl_{17}NZr$: C 35.4, H 3.15, N 1.2; found: C 36.2, H 3.6, N 2.4.

Synthesis of $[NBu_4][Hf(C_6Cl_5)_3Cl_2]$ (6): Using the procedure just described for synthesizing **5**, **6** was prepared by using $HfCl_4$ (2.03 g, 6.34 mmol), LiC_6Cl_5 (ca. 45 mmol), and $[NBu_4]Br$ (2.04 g, 6.34 mmol). Complex **6** was obtained as a brown solid (5.20 g, 4.20 mmol; 66% yield). Crystals suitable for X-ray diffraction analysis were obtained by slow diffusion of a layer of *n*-hexane (15 mL) into a solution of **6** (35 mg) in CH_2Cl_2 (6 mL) at −30 °C. ^{13}C NMR ([^{2}H]dichloromethane, −20 °C):[72] δ = 191.81 (*ipso*-C), 137.72, 131.94, 131.68 (*p*-C); IR (KBr): $\tilde{\nu}_{max}$ = 1509 (m), 1480 (m), 1470 (m), 1396 (m), 1381 (w), 1324 (m), 1316 (s), 1284 (vs), 1218 (w), 1167 (w), 1148 (w), 1070 (s), 878 (w; NBu_4^+), 834 (s; C_6Cl_5: X-sensitive vibr.),[8] 739 (w; NBu_4^+), 670 (s), 295 cm^{-1} (m; Hf−Cl); MS (FAB): *m/z*: 991 $[Hf(C_6Cl_5)_3Cl_2]^-$, 779 $[Hf(C_6Cl_5)_2Cl_3]^-$, 567 $[Hf(C_6Cl_5)Cl_4]^-$; elemental analysis calcd (%) for $C_{34}H_{36}Cl_{17}HfN$: C 32.9, H 2.9, N 1.1; found: C 33.5, H 3.5, N 1.0.

X-ray structure determinations: Crystal data and other details of the structure analyses are presented in Table 8. Suitable crystals of **1′**–**6** were obtained as indicated in each synthetic procedure. Crystals were mounted at the end of a glass fibre and held in place with either epoxy adhesive or a fluorinated oil.

1′: unit cell dimensions were determined using 25 centered reflections in the range $20.4 < 2\theta < 31.3°$. All diffraction measurements were made on an Enraf–Nonius CAD-4 diffractometer in a quarter of reciprocal space for $4.0 < 2\theta < 50.0°$ by ω scans. An absorption correction was applied on the basis of 422 azimuthal scan data (maximum and minimum transmission coefficients were 0.792 and 0.747).

2·2 CH_2Cl_2: unit cell dimensions were initially determined from the positions of 43 reflections in 60 intensity frames measured at 0.3° intervals in ω and subsequently refined on the basis of positions for 2483 reflections from the main data set. A hemisphere of data was collected on a Bruker SMART APEX diffractometer based on three ω-scan runs (starting ω = −28°) at values ϕ = 0°, 90°, and 180° with the detector at 2θ = 28°. For each of these runs, frames were collected at 0.3° intervals and 10 s per frame. The diffraction frames were integrated using the SAINT package[73] and corrected with SADABS.[74]

3·0.75 CH_2Cl_2·0.5 C_6H_{14}: unit cell dimensions were initially determined from the positions of 60 reflections in 90 intensity frames measured at 0.3° intervals in ω and subsequently refined on the basis of positions for 2052 reflections from the main data set. A hemisphere of data was collected on a Bruker SMART APEX diffractometer based on three ω-scan runs (starting ω = −28°) at values ϕ = 0°, 90°, and 180° with the detector at 2θ = 28°. For each of these runs, frames were collected at 0.3° intervals and 20 s per frame. The diffraction frames were integrated using the SAINT package[73] and corrected with SADABS.[74]

4·0.25 C_2Cl_4: unit cell dimensions were initially determined from the positions of 42 reflections in 90 intensity frames measured at 0.3° intervals in ω and subsequently refined on the basis of positions for 1149 reflections from the main data set. A hemisphere of data was collected on a Bruker SMART APEX diffractometer based on three ω-scan runs (starting ω = −28°) at values ϕ = 0°, 90°, and 180° with the detector at 2θ = 28°. For each of these runs, frames were collected at 0.3° intervals and 10 s per frame. The diffraction frames were integrated using the SAINT package[73] and corrected with SADABS.[74]

5·0.75CH_2Cl_2: unit cell dimensions were determined using 25 centered reflections in the range $22.0 < 2\theta < 30.5°$. All diffraction measurements were made on an Enraf–Nonius CAD-4 diffractometer in a quarter of reciprocal space for $4.0 < 2\theta < 50.0°$ by ω scans. An absorption correction was applied on the basis of 407 azimuthal scan data (maximum and minimum transmission coefficients were 0.845 and 0.745).

6·0.5 CH_2Cl_2: unit cell dimensions were determined using 25 centered reflections in the range $22.2 < 2\theta < 31.2°$. All diffraction measurements were made on an Enraf–Nonius CAD-4 diffractometer in a quarter of reciprocal space for $4.0 < 2\theta < 50.0°$ by ω scans. An absorption correction was applied on the basis of 492 azimuthal scan data (maximum and minimum transmission coefficients were 0.854 and 0.664).

The structures were solved by Patterson and Fourier methods. All refinements were carried out using the programs SHELXL-93 (for **1′**)[75] and SHELXL-97.[76] All non-hydrogen atoms were assigned anisotropic displacement parameters and refined without positional constraints except as noted below. All hydrogen atoms were constrained to idealized geometries and assigned isotropic displacement parameters 1.2 times the U_{iso} value of their attached carbon atoms (1.5 times for methyl hydrogen atoms). For **2**·CH_2Cl_2 no H atoms were added to the solvent molecule. For **3**·0.75 CH_2Cl_2·0.5 C_6H_{14} two dichloromethane molecules were found at 0.5 and 0.25 occupancies, respectively; the solvent atoms were refined with isotropic displacement parameters and no H atoms were added; the *n*-hexane molecule is located on an inversion center, so only half the molecule is found in the asymmetric unit. In the solvent area of **4**·0.25 C_2Cl_4 only two Cl atoms could be located, they being refined with isotropic displacement parameters. For **5**·0.75 CH_2Cl_2 the solvent molecules were found to be disordered over two positions sharing the C atom; the occupancy of the Cl atoms within each set was 0.60 and 0.15, respectively; a common set of thermal anisotropic displacement parame-

Table 8. Crystal data and structure refinement for compounds **1′**–**6**.

	1′	**2**·2CH_2Cl_2	**3**·0.75CH_2Cl_2·0.5C_6H_{14}	**4**·0.25C_2Cl_4	**5**·0.75CH_2Cl_2	**6**·0.5CH_2Cl_2
formula	$C_{41}H_{38}Cl_{22}LiO_4Ti$	$C_{26}H_4Cl_{24}Ti$	$C_{63.75}H_{38.5}Cl_{21.5}NP_2Tl$	$C_{24.5}Cl_{21}Sn$	$C_{34.75}H_{37.5}Cl_{18.5}NZr$	$C_{34.5}H_{37}Cl_{18}HfN$
M_r [g mol^{-1}]	1429.45	1214.99	1846.94	1157.39	1216.20	1282.24
T [K]	150(2)	100(2)	100(2)	173(2)	150(2)	150(2)
λ [pm]	71.073	71.073	71.073	71.073	71.073	71.073
crystal system	monoclinic	tetragonal	monoclinic	monoclinic	monoclinic	monoclinic
space group	$C2/c$	$P\bar{4}2_1c$	$P2_1/c$	$C2/c$	$P2_1/c$	$P2_1/c$
a [pm]	1674.8(5)	1498.93(14)	2250.7(2)	2956.6(4)	2240.7(2)	2239.2(6)
b [pm]	1915.46(15)	1498.93(14)	969.60(9)	1441.05(18)	1734.96(16)	1732.99(18)
c [pm]	1758.0(2)	869.98(12)	3288.7(3)	2419.8(3)	1240.0(2)	1237.5(2)
β [°]	91.58(3)	90	92.772(2)	124.956(2)	91.739(17)	91.757(15)
V [nm^3]	5.6376(18)	1.9547(4)	7.1685(12)	8.4499(19)	4.8184(11)	4.8000(17)
Z	4	2	4	8	4	4
ρ [g cm^{-3}]	1.684	2.064	1.711	1.820	1.677	1.774
μ [mm^{-1}]	1.235	1.886	3.140	1.953	1.283	3.204
F(000)	2860	1180	3618	4432	2430	2516
2θ range [°]	4.0–50.0 ($+h$, $+k$, $\pm l$)	3.8–50.0 ($\pm h$, $\pm k$, $\pm l$)	3.0–50.0 ($\pm h$, $\pm k$, $\pm l$)	4.4–49.4 ($\pm h$, $\pm k$, $\pm l$)	4.0–50.0 ($\pm h$, $-k$, $+l$)	4.0–50.0 ($\pm h$, $-k$, $+l$)
final R indices [$I>2\sigma(I)$][a]						
R_1	0.0484	0.0409	0.0723	0.0642	0.0582	0.0764
wR_2	0.1202	0.1106	0.1603	0.1306	0.1405	0.1829
R indices (all data)						
R_1	0.0761	0.0504	0.1531	0.1346	0.1247	0.1087
wR_2	0.1385	0.1156	0.1951	0.1514	0.1718	0.1964
goodness-of-fit on F^2 [b]	1.037	1.020	0.952	0.859	1.010	1.160

[a] $R_1 = \Sigma(|F_o|-|F_c|)/\Sigma|F_o|$; $wR_2 = [\Sigma w(F_o^2-F_c^2)^2/\Sigma w(F_c^2)^2]^{1/2}$; $w = [\sigma^2(F_o^2) + (g_1P)^2 + g_2P]^{-1}$; $P = (1/3)\cdot[\max\{F_o^2,0\}+2F_c^2]$. [b] Goodness-of-fit $= [\Sigma w(F_o^2-F_c^2)^2/(n_{obs}-n_{param})]^{1/2}$.

ters was used for the Cl atoms of each component of the disorder. For **6**·0.5CH_2Cl_2 a common set of thermal anisotropic displacement parameters was used for the solvent atoms and another one for the N and α-C atoms of the $[NBu_4]^+$ ion. Full-matrix least-squares refinement of these models against F^2 converged to final residual indexes given in Table 8. Lorentz and polarization corrections were applied for all the structures.

CCDC-172710, and CCDC-229859–CCDC-229863 contain the supplementary crystallographic data for this paper. These data can be obtained free of charge via www.ccdc.cam.ac.uk/conts/retrieving.html (or from the Cambridge Crystallographic Data Centre, 12 Union Road, Cambridge CB2 1EZ, UK; fax: (+44) 1223-336-033; or deposit@ccdc.cam.ac.uk).

EPR measurements: EPR data were obtained in a Bruker ESP380 spectrometer. The magnetic field was measured with a Bruker ER035M gaussmeter. A Hewlett–Packard HP5350B frequency counter was used to determine the microwave frequency.

Acknowledgement

This work has been supported by the Spanish MCYT (DGI)/FEDER (Projects BQU2002-03997-CO2-02 and BQU2002–00554) and the Gobierno de Aragón (Grupo Consolidado: Química Inorgánica y de los Compuestos Organometálicos). The Gobierno de Aragón is also acknowledged for a grant to M. A. G.-M. We are indebted to Prof. Dr. S. Alvarez (Universitat de Barcelona) for kindly providing values of continuous symmetry measure.

[1] J. E. Huheey, E. A. Keiter, R. L. Keiter, *Inorganic Chemistry*, 4th ed., HarperCollins College, New York, **1993**, pp. 624–630; M. Laing in *Coordination Chemistry—A Century of Progress, ACS Symposium Series 565* (Ed.: G. B. Kauffman), American Chemical Society, Washington DC, **1994**, chapter 15, pp. 193–198.
[2] N. V. Sidgwick, *The Electronic Theory of Valency*, Oxford University Press, London, **1927** (Impression of **1932**), chapter 10, pp. 163–184.
[3] R. B. King, *Coord. Chem. Rev.* **2000**, *197*, 141.
[4] C. A. Tolman, *Chem. Soc. Rev.* **1972**, *1*, 337.
[5] R. Poli, *Chem. Rev.* **1996**, *96*, 2135.
[6] P. R. Mitchell, R. V. Parish, *J. Chem. Educ.* **1969**, *46*, 811.
[7] P. J. Alonso, J. Forniés, M. A. García-Monforte, A. Martín, B. Menjón, *Chem. Commun.* **2002**, 728.
[8] a) R. Usón, J. Forniés, *Adv. Organomet. Chem.* **1988**, *28*, 219; b) E. Maslowsky, Jr., *Vibrational Spectra of Organometallic Compounds*, Wiley, New York, **1977**, pp.437–442.
[9] G. M. Barrow, S. Searles, *J. Am. Chem. Soc.* **1953**, *75*, 1175; L. J. Bellamy, *The Infra-Red Spectra of Complex Molecules*, *Vol. 1*, 3rd ed., Chapman and Hall, London, **1975**, Ch. 7, pp. 129–140.
[10] K. J. R. Rosman, P. D. P. Taylor, *Pure Appl. Chem.* **1998**, *70*, 217.
[11] W. R. Entley, C. R. Treadway, S. R. Wilson, G. S. Girolami, *J. Am. Chem. Soc.* **1997**, *119*, 6251; W. W. Lukens, Jr., M. R. Smith III, R. A. Andersen, *J. Am. Chem. Soc.* **1996**, *118*, 1719, and references therein.
[12] V. Dimitrov, K.-H. Thiele, D. Schenke, *Z. Anorg. Allg. Chem.* **1985**, *527*, 85.
[13] D. Schenke, K.-H. Thiele, *J. Organomet. Chem.* **1990**, *382*, 109.
[14] W. A. Sheppard, *J. Am. Chem. Soc.* **1970**, *92*, 5419.
[15] N. G. Connelly, W. E. Geiger, *Chem. Rev.* **1996**, *96*, 877.
[16] The ability of $[SbCl_6]^-$ to become involved in oxidation processes of aromatic hydrocarbons, aromatic amines, phenoxide ions, I^-, ferrocene, and metal–metal multiply bonded complexes of technetium has been documented. In some instances, cation-mediated formation of transient $SbCl_5$ as the active oxidation agent has been suggested. See: F. A. Cotton, S. C. Haefner, A. P. Sattelberger, *Inorg. Chim. Acta* **1998**, *271*, 187; R. Rathore, A. S. Kumar, S. V. Lindeman, J. K. Kochi, *J. Org. Chem.* **1998**, *63*, 5847; R. Rathore, J. K. Kochi, *J. Org. Chem.* **1995**, *60*, 4399; G. W. Cowell, A. Ledwith, A. C. White, H. J. Woods, *J. Chem. Soc. B* **1970**, 227.
[17] M. Bochmann in *Comprehensive Organometallic Chemistry II, Vol. 4* (Eds.: E. W. Abel, F. G. A. Stone, G. Wilkinson), Elsevier Science, Oxford, UK, **1995**, Ch. 4, pp. 221–271; M. Bochmann in *Comprehensive Organometallic Chemistry II, Vol. 4* (Eds.: E. W. Abel, F. G. A. Stone, G. Wilkinson), Elsevier Science, Oxford, UK, **1995**, Ch. 5, pp. 273–431; M. Botrill, P. D. Gavens, J. McMeeking in *Comprehensive Organometallic Chemistry, Vol. 3* (Eds.: G. Wilkinson, F. G. A. Stone, E. W. Abel), Pergamon, Oxford, UK, **1982**, Section 22.2, pp. 281–329; M. Botrill, P. D. Gavens, J. W. Kelland, J. McMeeking in *Comprehensive Organometallic Chemistry, Vol. 3* (Eds.: G. Wilkinson, F. G. A. Stone, E. W. Abel), Pergamon, Oxford,

UK, **1982**, Section 22.3, pp. 331–431; M. Botrill, P. D. Gavens, J. W. Kelland, J. McMeeking in *Comprehensive Organometallic Chemistry, Vol. 3* (Eds.: G. Wilkinson, F. G. A. Stone, E. W. Abel), Pergamon, Oxford, UK, **1982**, Section 22.4, pp. 433–474.

[18] W. J. Pope, S. J. Peachey, *J. Chem. Soc. Trans.* **1909**, *95*, 571; W. J. Pope, S. J. Peachey, *Proc. Chem. Soc. London* **1907**, *23*, 86.

[19] D. F. Herman, W. K. Nelson, *J. Am. Chem. Soc.* **1953**, *75*, 3877; D. F. Herman, W. K. Nelson, *J. Am. Chem. Soc.* **1952**, *74*, 2693.

[20] For a recent review on the use of non-metallocene transition-metal derivatives (including Cp-free compounds) in olefin polymerization, see: V. C. Gibson, S. K. Spitzmesser, *Chem. Rev.* **2003**, *103*, 283. Further examples are given where appropriate in the discussion.

[21] See for instance: C. R. Landis, T. Cleveland, T. K. Firman, *J. Am. Chem. Soc.* **1998**, *120*, 2641; C. R. Landis, T. K. Firman, D. M. Root, T. Cleveland, *J. Am. Chem. Soc.* **1998**, *120*, 1842.

[22] H. Rau, J. Müller, *Z. Anorg. Allg. Chem.* **1975**, *415*, 225; J. Müller, H. Rau, P. Zdunneck, K.-H. Thiele, *Z. Anorg. Allg. Chem.* **1973**, *401*, 113; K.-H. Thiele, K. Milowski, P. Zdunneck, J. Müller, H. Rau, *Z. Chem.* **1972**, *12*, 186.

[23] S. Kleinhenz, K. Seppelt, *Chem. Eur. J.* **1999**, *5*, 3573.

[24] U. Zucchini, E. Albizzati, U. Giannini, *J. Organomet. Chem.* **1971**, *26*, 357; U. Giannini, U. Zucchini, *J. Chem. Soc. D* **1968**, 940.

[25] a) W. Mowat, G. Wilkinson, *J. Chem. Soc. Dalton Trans.* **1973**, 1120; b) P. J. Davidson, M. F. Lappert, R. Pearce, *J. Organomet. Chem.* **1973**, *57*, 269; c) W. Mowat, G. Wilkinson, *J. Organomet. Chem.* **1972**, *38*, C35.

[26] M. R. Collier, M. F. Lappert, R. Pearce, *J. Chem. Soc. Dalton Trans.* **1973**, 445.

[27] W. Seidel, I. Bürger, *Z. Chem.* **1977**, *17*, 185.

[28] B. K. Bower, H. G. Tennent, *J. Am. Chem. Soc.* **1972**, *94*, 2512; see also ref. [12].

[29] T. J. Groshens, C. K. Lowe-Ma, R. C. Scheri, R. Z. Dalbey, *Mater. Res. Soc. Symp. Proc.* **1993**, *282*, 299; G. S. Girolami, J. A. Jensen, D. M. Pollina, C. M. Allocca, A. E. Kaloyeros, W. S. Williams, *J. Am. Chem. Soc.* **1987**, *109*, 1579.

[30] H. J. Berthold, G. Groh, *Z. Anorg. Allg. Chem.* **1963**, *319*, 230.

[31] K.-H. Thiele, J. Müller, *J. Prakt. Chem.* **1968**, *38*, 147; K. Clauss, C. Beermann, *Angew. Chem.* **1959**, *71*, 627. For problems associated with reacting titanium(IV) tetrahalides with MeMgCl in nonpolar solvents, see: K.-H. Thiele, K. Jacob, *Z. Anorg. Allg. Chem.* **1968**, *356*, 195. For the ascription of the stability of "$TiMe_4$" in Et_2O solution to formation of $TiMe_4{\cdot}n(OEt_2)$ adducts, see: K.-H. Thiele, J. Müller, *Z. Anorg. Allg. Chem.* **1968**, *362*, 113.

[32] a) I. W. Bassi, G. Allegra, R. Scordamaglia, G. Chioccola, *J. Am. Chem. Soc.* **1971**, *93*, 3787; b) G. R. Davies, J. A. J. Jarvis, B. T. Kilbourn, *J. Chem. Soc. D* **1971**, 1511.

[33] C. Tedesco, A. Immirzi, A. Proto, *Acta Crystallogr. Sect. B* **1998**, *54*, 431; G. R. Davies, J. A. J. Jarvis, B. T. Kilbourn, A. J. P. Pioli, *J. Chem. Soc. D* **1971**, 677; see also ref. [32b].

[34] G. K. Barker, M. F. Lappert, J. A. K. Howard, *J. Chem. Soc. Dalton Trans.* **1978**, 734; G. K. Barker, M. F. Lappert, *J. Organomet. Chem.* **1974**, *76*, C45. About the isolation and stability of $[Ti(CH_2Ph)_3]$, see: A. Röder, J. Scholz, K.-H. Thiele, *Z. Anorg. Allg. Chem.* **1983**, *505*, 121.

[35] M. Llunell, D. Casanova, J. Cirera, J. M. Bofill, P. Alemany, S. Alvarez, M. Pinsky, D. Avnir, SHAPE (version 1.1), Universitat de Barcelona (Spain) and The Hebrew University of Jerusalem (Israel).

[36] One of the most plausible attempts to accurately describe real coordination entities in terms of regular geometric polyhedra has been the introduction of the continuous symmetry measure, *S*. Following its mathematical definition, deviations from a given polyhedron in bond lengths as well as in interbond angles both contribute to increase the *S* value. Thus, the smaller the value of *S*, the better the agreement between the real molecule and the suggested model, $S = 0$ for perfect coincidence: M. Pinsky and D. Avnir, *Inorg. Chem.* **1998**, *37*, 5575. This parameter has been successfully applied to several coordination geometries: a) J. Cirera, P. Alemany, S. Alvarez, *Chem. Eur. J.* **2004**, *10*, 190; b) D. Casanova, P. Alemany, J. M. Bofill, S. Alvarez, *Chem. Eur. J.* **2003**, *9*, 1281; c) S. Alvarez, D. Avnir, M. Llunell, M. Pinsky, *New J. Chem.* **2002**, *26*, 996; d) S. Alvarez, M. Llunell, *J. Chem. Soc. Dalton Trans.* **2000**, 3288.

[37] G. J. Olthof, F. van Bolhuis, *J. Organomet. Chem.* **1976**, *122*, 47.

[38] J. D. Zeinstra, J. H. Teuben, F. Jellinek, *J. Organomet. Chem.* **1979**, *170*, 39.

[39] R. K. Minhas, L. Scoles, S. Wong, S. Gambarotta, *Organometallics* **1996**, *15*, 1113.

[40] J. M. Rosset, C. Floriani, M. Mazzanti, A. Chiesi-Villa, C. Guastini, *Inorg. Chem.* **1990**, *29*, 3991.

[41] R. W. Chesnut, L. D. Durfee, P. E. Fanwick, I. P. Rothwell, K. Folting, J. C. Huffman, *Polyhedron* **1987**, *6*, 2019.

[42] F. Guérin, J. C. Stewart, C. Beddie, D. W. Stephan, *Organometallics* **2000**, *19*, 2994.

[43] D. P. Steinhuebel, S. J. Lippard, *Inorg. Chem.* **1999**, *38*, 6225.

[44] C. O. Kienitz, C. Thöne, P. G. Jones, *Acta Crystallogr. Sect. C* **1996**, *52*, 2402.

[45] R. J. Gillespie, I. Hargittai, *The VSEPR model of molecular geometry*, Allyn and Bacon, Boston, **1991**, p. 171.

[46] G. L. Heard, R. J. Gillespie, D. W. H. Rankin, *J. Mol. Struct.* **2000**, *520*, 237.

[47] P. J. Alonso, J. Forniés, M. A. García-Monforte, A. Martín, B. Menjón, C. Rillo, *Chem. Eur. J.* **2002**, *8*, 4056; P. J. Alonso, L. R. Falvello, J. Forniés, M. A. García-Monforte, A. Martín, B. Menjón, G. Rodríguez, *Chem. Commun.* **1998**, 1721.

[48] M. P. García, M. V. Jiménez, A. Cuesta, C. Siurana, L. A. Oro, F. J. Lahoz, J. A. López, M. P. Catalán, A. Tiripicchio, M. Lanfranchi, *Organometallics* **1997**, *16*, 1026.

[49] J. Forniés, B. Menjón, R. M. Sanz-Carrillo, M. Tomás, N. G. Connelly, J. G. Crossley, A. G. Orpen, *J. Am. Chem. Soc.* **1995**, *117*, 4295.

[50] P. J. Alonso, J. Forniés, M. A. García-Monforte, A. Martín, B. Menjón, *Chem. Commun.* **2001**, 2138.

[51] T. Głowiak, R. Grobelny, B. Jeżowska-Trzeblatowska, G. Kreisel, W. Seidel, E. Uhlig, *J. Organomet. Chem.* **1978**, *155*, 39.

[52] R. Usón, A. Laguna, J. A. Abad, *J. Organomet. Chem.* **1980**, *194*, 265.

[53] a) H. Gilman, S.-Y. Sim, *J. Organomet. Chem.* **1967**, *7*, 249; b) inconclusive Mössbauer spectroscopic data for the tin species were also reported: M. Cordey-Hayes, R. D. W. Kemmitt, R. D. Peacock, G. D. Rimmer, *J. Inorg. Nucl. Chem.* **1969**, *31*, 1515.

[54] L. Fajarí, L. Juliá, J. Riera, E. Molins, C. Miravitlles, *J. Organomet. Chem.* **1990**, *381*, 321.

[55] a) M. A. Lloyd, C. P. Brock, *Acta Crystallogr. Sect. B* **1997**, *53*, 780; b) N. A. Ahmed, A. I. Kitaigorodsky, K. V. Mirskaya, *Acta Crystallogr. Sect. B* **1971**, *27*, 867.

[56] a) V. K. Belsky, A. A. Simonenko, V. O. Reikhsfeld, I. E. Saratov, *J. Organomet. Chem.* **1983**, *244*, 125; b) P. C. Chieh, *J. Chem. Soc. Dalton Trans.* **1972**, 1207.

[57] A. Karipides, C. Forman, R. H. P. Thomas, A. T. Reed, *Inorg. Chem.* **1974**, *13*, 811.

[58] C. A. Tolman, *J. Am. Chem. Soc.* **1970**, *92*, 2953; see also ref. [14].

[59] A. Mendía, E. Cerrada, E. J. Fernández, A. Laguna, M. Laguna, *J. Organomet. Chem.* **2002**, *663*, 289.

[60] J. Blümel, B. Werner, T. Kräuter, B. Neumüller, *Z. Anorg. Allg. Chem.* **1997**, *623*, 309.

[61] M. J. Nelsen, G. S. Girolami, *J. Organomet. Chem.* **1999**, *585*, 275.

[62] The angular structural parameter, τ, has been defined as an index of trigonality. It takes continuous values between 0 and 1 ($0 \leq \tau \leq 1$) with the lower and upper limits denoting ideal *SPY*-5 and *TBPY*-5 geometries, respectively. For the definition and use of this geometric descriptor of five-coordinate molecules see: A. W. Addison, T. N. Rao, J. Reedijk, J. van Rijn, G. C. Verschoor, *J. Chem. Soc. Dalton Trans.* **1984**, 1349; see also ref. [36d].

[63] K. Prout, T. S. Cameron, R. A. Forder, S. R. Critchley, B. Denton, G. V. Rees, *Acta Crystallogr. Sect. B* **1974**, *30*, 2290.

[64] W. Clegg, L. Horsburgh, D. M. Lindsay, R. E. Mulvey, *Acta Crystallogr. Sect. C* **1998**, *54*, 315.

[65] L. H. McAlexander, L. T. Li, Y. H. Yang, J. L. Pollitte, Z. L. Xue, *Inorg. Chem.* **1998**, *37*, 1423.

[66] D. J. Cardin, M. F. Lappert, C. L. Raston, *Chemistry of Organo-Zirconium and -Hafnium Compounds*, Ellis Horwood, Chichester, UK, **1986**; W. E. Hunter, J. L. Atwood, G. Fachinetti, C. Floriani, *J. Organomet. Chem.* **1981**, *204*, 67.

[67] L. E. Manzer, *Inorg. Synth.* **1982**, *21*, 135.

[68] B. Heyn, B. Hipler, G. Kreisel, H. Schreer, D. Walther, *Anorganische Synthesechemie*, Springer, Berlin, Germany, **1986**, p. 15.

[69] M. D. Rausch, F. E. Tibbetts, H. B. Gordon, *J. Organomet. Chem.* **1966**, *5*, 493.
[70] J. K. Ruff, W. J. Schlientz, *Inorg. Synth.* **1974**, *15*, 84.
[71] External [^{2}H]benzene was used as the lock signal.
[72] Resonances from the NBu_4^+ ion have been omitted.
[73] SAINT, version 6.2, Bruker Analytical X-ray Systems, Madison WI, **1999**.
[74] G. M. Sheldrick, SADABS empirical absorption program, version 2.03, University of Göttingen, Göttingen, Germany, **1996**.
[75] G. M. Sheldrick, SHELXL-93, Program for the Refinement of Crystal Structures from Diffraction Data, University of Göttingen, Göttingen, Germany, **1993**.
[76] G. M. Sheldrick, SHELXL-97, Program for the Refinement of Crystal Structures from Diffraction Data, University of Göttingen, Göttingen, Germany, **1997**.

Received: February 11, 2004
Published online: July 9, 2004

